First-Principles Study of Carbon Chemisorption on γ-Fe(111) Surface

Y.W. Hua and G. Jiang*
Institute of atomic and molecular physics, Sichuan University, Chengdu, P. R. China

Y.L. Liu
College of electrical and information engineering, Southwest University for Nationalities, Chengdu, P. R. China

J. Chen
National Key Laboratory for Surface Physics and Chemistry, Mianyang, P. R. China
(Received on 28 October, 2009)

In order to study the interaction between γ-Fe and carbon, the geometry structures, surface relaxations, adsorption energies and electronic structures for carbon chemisorption at four different adsorption sites on γ-Fe(111) surface at a monolayer coverage of 1 were studied using density functional theory. The electronic structures were compared with the chemisorption of carbon on nickel (111) at the fcc hollow site. Based on the computational adsorption energies, the relative stabilities were described as follows: hcp hollow ≈ fcc hollow > top-on site, whereas the atomic carbon can not occupy the bridge sites stably. The partial density of states indicated the strong C(2p)-Fe(3d, 4s+p) and the wide C(2s+p)-Fe(3d) ionic bonds, which largely confined the electrons of the surface iron. Accordingly, the number of orbitals at the Fermi level for the iron in the surface is obviously less than that in the subsurface. Moreover, comparing the carbon chemisorptions on γ-Fe and nickel surface at the fcc hollow site, one could see that the number of orbitals at the Fermi level for carbon adsorbed on γ-Fe(111) is less than on Ni(111) surface. This could imply the weaker catalysis of γ-Fe than nickel for carbon atom.

Keywords: Density functional theory; adsorption energy; partial density of state; electronic structure.

1. INTRODUCTION

Chemisorption supplies useful theoretical evidence for studying the interaction between catalysts and reactants. Understanding the interaction of carbon with the transition-metal surface, and in particular with iron surface, is of primary importance as this system can be involved in many processes such as metallurgy, corrosion and catalysis [1,2,3]. It has long been known that iron, cobalt and nickel form an interesting subset of the metal catalysts [4],especially iron acts as a catalyst in the Boudard and Fischer-Trpsch reactions [5,6,7]. The chemisorption of C on Ni and Co surfaces had been studied by Klinke and Liu *et al.* [8,9,10]. Therefore, there is significant industrial and fundamental scientific motivation to understand some elementary processes such as chemisorption of C on Fe surfaces.

Due to the importance of metal catalyst, many investigations of chemisorptions on Fe have been performed, especially for the body-centered cubic (bcc) α-Fe at normal temperatures and pressures. The dissociation chemisorption of CO molecule on α-Fe (100), (710), (310) and (211) surface were studied by Sorescu[11,12] and Borthwick[13], respectively, with density functional theory (DFT). Also theoretical studies of C chemisorption on α-Fe(100), (110), and (111) surfaces along with the experimental studies of NO, CO, C and O chemisorptions on Fe(111) surfaces had been performed to evaluate their interactions [14-18]. However, for the face-centered cubic (fcc) γ-Fe at high temperatures and a wide pressure range [19], theoretical and experimental studies were scarce, available only for an experimental study of the reaction between coadsorbed NO and CO on ultra-thin γ-Fe films grown on Rh(100) surface by Egawa *et al.*[20]. In fact, the investigations on γ-Fe are quite important. For example, the common pressures and temperatures of synthesizing diamond in metal-carbon system are 5.0 to 5.8 GPa and 1500 to 1750 K [21], respectively, at which Fe has a stable fcc structure [19].

In the present work, chemisorption models of C on γ-Fe(111)-(1×1) at a monolayer (ML) coverage of 1 were built. The atomic geometries, relaxations, adsorption energies and electronic structures of C adsorbed at four different adsorption sites were calculated. Then, the different adsorption energies were compared to determine the most energetically favorable site, and the partial density of states (PDOS) were analyzed to recover the electronic structure influence of C on γ-Fe.

2. THEORETICAL METHODS AND MODELS

The Cambridge Serial Total Energy Package (CASTEP) in Material Studio (MS) [22] program was used in our work, which is a DFT code with plane-wave basis set. All of the calculations were performed using the ultrasoft pseudopotentials [23], including non-linear core corrections (NLCC) in the case of Fe [24]. Electronic exchange and correlation effects were included within the generalized gradient approximation (GGA) [25] with a specific functional PW91 proposed by Perdew *et al.* for the geometry optimization calculations [26]. Once optimized geometries were obtained, we held these fixed and replaced the PW91 functional with the revised Perdew-Burke-Ernzerhoff (RPBE) functional [27] to obtain a more accurate picture of relative and absolute adsorption energies. That is because the PW91 functional can give reliable optimized geometry [13,28,29], while the RPBE systematically improves the atomization energies for

*E-mail: gjiang@scu.edu.cn

a large database of small molecules and the chemisorption energies of atoms and molecules on a transition-metal surface [13,28,30]. Geometry optimization in RPBE even may result either in lack of a local minimum or the existence of a very shallow minimum further away from the surface [28]. The widely used slab model was employed to build our surface models.

The bulk Fe lattice parameter was firstly obtained utilizing periodic boundary conditions appropriate to a primitive unit cell. Acceptable convergences of the plane-wave energy cutoff and the Monkhorst-Pack k-point grid within the Brillouin zone were 320.0 eV and $20\times20\times20$, respectively, yielding a conventional lattice parameter of 0.344 nm. The computational value agreed well with Haglund's theoretical value of 0.343 nm[31], but it made a slight difference with the experimental value of 0.365 nm[32-34]. For the γ-Fe exists at such high temperatures [19], the difference may be due to the thermal expansion effect. In order to obtain the more realistic adsorption energies and PDOS, the experimental lattice parameter 0.365 nm was adopted to build the surface models. The metal substrate was represented by a five-layer slab for Fe(111) separated by a 1.2 nm thick vacuum region. In order to reduce the computational demand, the surface reconstruction was not considered in the calculations, since the models were based on the (1×1) unit cells. Subsequently, the models of C adsorption on γ-Fe(111) surface at 1 ML were built as shown in Fig.1.Four different adsorption sites, namely the top-on, fcc hollow, hcp hollow and bridge site, were optimized firstly. It turned out that the atomic C can not occupy the bridge site stably. Accordingly, the bridge site adsorption model was not shown in Fig. 1.

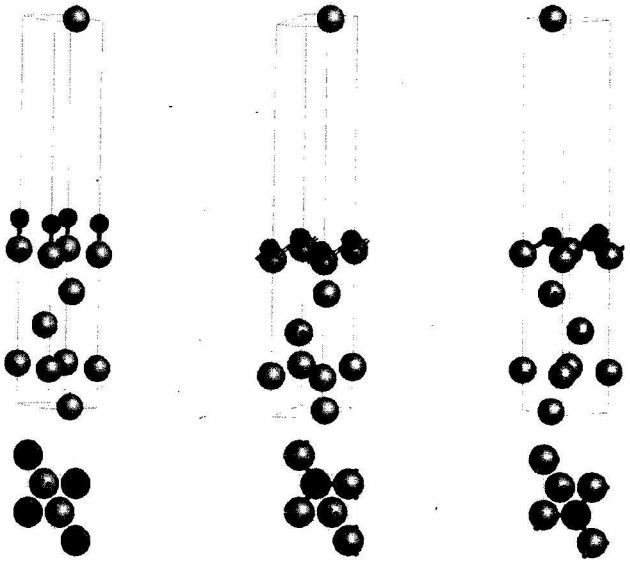

FIG. 1: The side and top view of the Fe(111)-p (1×1)-C adsorption system at 1 ML with the C atom adsorbed at the top-on (a), fcc hollow (b) and hcp hollow (c) sites. The white and black spheres represent Fe and C atoms respectively.

During the geometry optimization of all the models, the surface unit cells constrained all the parameters of the bottom three layers of Fe atoms, while the adsorbates and the top two layers of the substrate were completely relaxed, and the lattice parameters were not optimized as well. According to our convergence test, the k-space was divided with the Monkhorst-Pack k-point grid of $16\times16\times1$ within the Brillouin zones of the adsorption models, and the plane-wave cutoff energy used was 330.0 eV. The scheme BFGS was used for geometry optimization [35]. Spin polarization was included in all the calculations. The convergence threshold for the total energy, maximum force, and maximum displacement were 0.00012 eV, 0.05 eV/nm, and 0.002 nm, respectively.

3. RESULTS AND DISCUSSION

3.1. Adsorption energies analysis

Firstly, the adsorption energies of C on Fe(111)-(1×1) surface for the various adsorption sites at 1 ML were calculated, and it was defined as shown in Eq. (1),

$$E_{ads} = E_{Fe} + E_C - E_{Fe:C} \tag{1}$$

Where, $E_{Fe:C}$ is the total energies of the adsorption systems, E_{Fe} is the energy of the Fe(111)-(1×1) clean surface, and E_C is the spin polarized energy of free adatom C, which is -147.459 eV. For the various adsorption sites, the calculated adsorption energies of C atom, the top-layer and the second-layer relaxations relative to the bulk interlayer distance d_0, the optimized distance between C and the top-layer, the optimized bond lengths of C-Fe along with bond angles of Fe-C-Fe were summarized in Table 1.

Tab. 1 Calculated adsorption energy, E_{ads} ; Top-layer relaxation,$\triangle d_{12}$; Second-layer relaxation,$\triangle d_{23}$; Optimized distance between C and the top-layer, D_{C-top} ; and optimized bond lengths of C-Fe along with bond angles of Fe-C-Fe, for C on

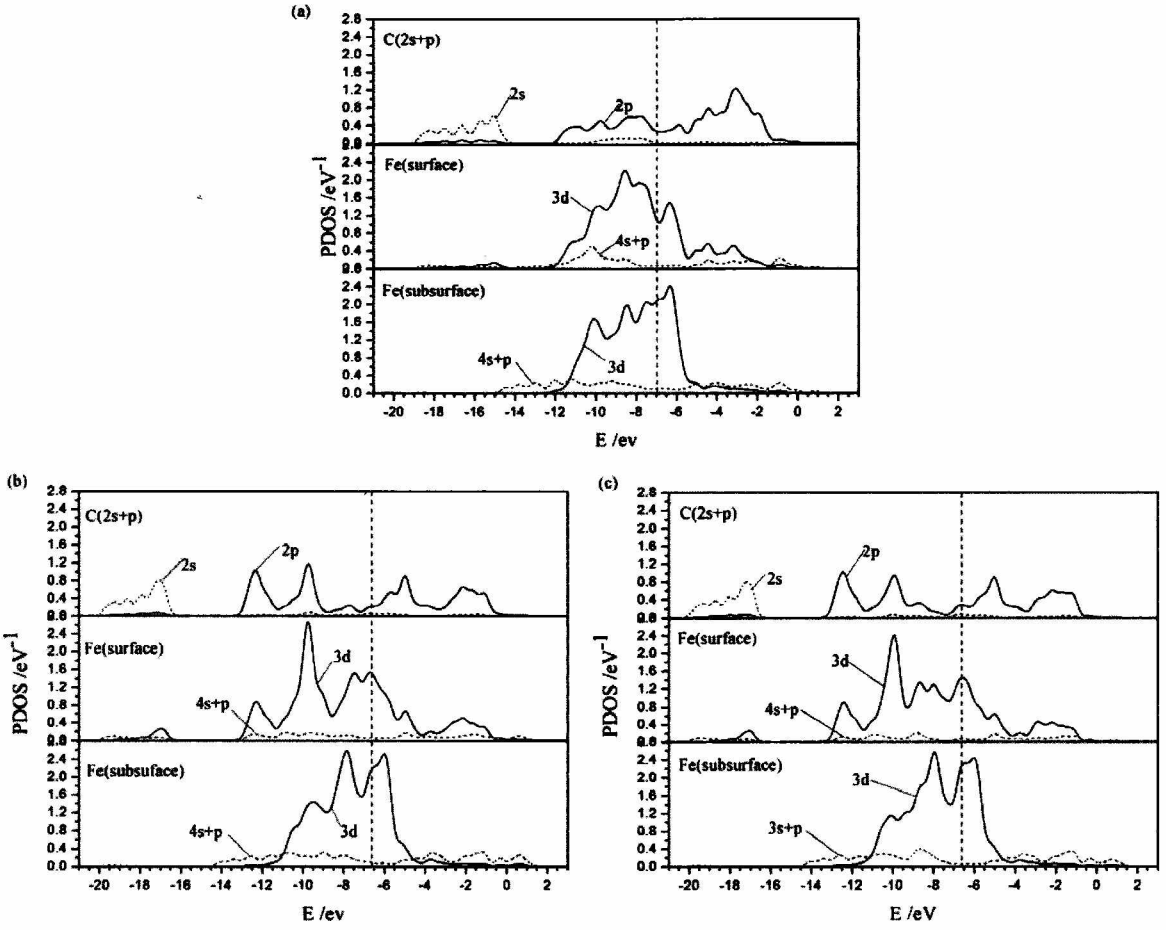

FIG. 2: Layer resolved partial density of state for the Fe(111)-p(1×1)-C system at 1 ML. (a) top-on site (b) fcc hollow site (c) hcp hollow site. The C(2s) and Fe(4s+p) orbital contributions are represented by dotted lines, while the C(2p) and Fe(3d) orbital contributions are represented by solid lines. The vertical dashed lines donate the Fermi level

Fe(111) surface at 1 ML at various adsorption sites.

Adsorption site	E_{ads}(eV)	$\triangle d_{12}(\%)$	$\triangle d_{23}(\%)$	D_{C-top}(nm)	Bond length(nm)	Bond angle(°)
Top-on	4.75	-3.08	12.23	0.163	0.163	0
Fcchollow	6.38	1.02	11.75	0.0948	0.177	93.93,93.93,93.94
Hcp hollow	6.52	-3.04	10.18	0.0947	0.177	94.00,94.00,93.95

As shown in table 1, the hcp hollow is the most energetically favorable site for C chemisorption on Fe(111) with a chemisorption energy of 6.52 eV, followed by the fcc hollow site and top-on site, with the chemisorption energies of 6.38 eV and 4.75 eV, respectively. We noted that the chemisorption energies for the fcc hollow and hcp hollow sites were very close and differed by only 0.14 eV. On the other hand, for the hcp hollow site, the distance of the carbon atom from the top layer has the lowest value of 0.0947 nm, and then the fcc hollow site of 0.0948 nm. This distance increased as the coordination of the carbon atom with the γ-Fe surface decreased, thus, the adsorption energies of C declined.

3.2. Electronic structure analysis

Electronic structure calculations[36] are essential for studying the microscopic quantum mechanical properties of solids, molecules and some nanoscale materials. PDOS provide an insight into the interactions between the adsorbates and the adsorbents. In order to illustrate the interaction between the γ-Fe surface and the adsorbate at various adsorption sites, the PDOS for the models in Fig. 1 were calculated as shown in Fig. 2. The Fermi energies were -6.930, -6.592 and -6.596 eV for the top-on, fcc hollow and hcp hollow sites, respectively. In the case of molecular bonding, the formation of distinct bonding states below the Fermi level and unoccupied antibonding states above the Fermi level were

expected. When C atoms were adsorbed at the top-on sites as shown in Fig. 2(a), ranging from -19.0 to -14.3 eV, there was a hyperdeep C(2s) band below the surface valence band, and a few C(2p) and surface Fe(3d, 4s+p) electrons could also be found, while no subsurface Fe orbitals were found at all. Therefore, although they were not obvious, the slight surface Fe(3d, 4s+p) orbitals in this range were induced by their interactions with the C(2s+p) orbitals. Moreover, in comparison with the subsurface Fe, the wide C(2s+p)-Fe(3d) ionic bond decreased the energy of the surface Fe to a great extent, which suggested a stronger confinement of electrons than the Fe-Fe metallic bond just below the Fermi level. Accordingly, the PDOS at the Fermi level for the surface Fe decreased. Similarly, based on the PDOS of the fcc and hcp hollow adsorption as shown in Fig. 2(b) and 2(c), the orbitals ranging from -20.1 to 16.3 eV also indicated that the slight surface Fe(3d, 4s+p) orbitals in this range were due to their interactions with the C(2s+p) orbitals. But the downward energy shift of about 1.0 eV illuminated a stronger C-Fe interaction than the top-on adsorption. Evident C(2p), Fe(3d) and slight Fe(4s+p) bands near -12.5 and -10.0 eV could be found simultaneously for the hollow site adsorption. Therefore, the strong C(2p)-Fe(3d, 4s+p) bonds have also been considered. PDOS for the fcc and hcp hollow adsorption were almost the same, but had some differences just below the Fermi level as shown in Fig. 2(b) and 2(c), which arised from the interaction between the adatom C(2p) and the subsurface Fe(3d, 4s+p) for the hcp hollow adsorption. Furthermore, one of the striking characters for the PDOS is the number of orbitals at the Fermi levels, which is an important criterion for the catalysis of Fe[9,10]. In comparison with Klinke's and our previous studies upon C chemisorptions on Ni(111) surface at the fcc hollow site at 1 ML[8,9], one could see that the number of orbitals at the Fermi level for C adsorbed on γ-Fe(111) surface at the same adsorption site and monolayer coverage was less than on the Ni(111) surface, relatively speaking, which could be attributed to the stronger C-Fe interactions. That could imply the weaker catalysis of γ-Fe than Ni for C atom.

4. CONCLUSIONS

In conclusion, we studied atomic carbon adsorption on γ-Fe(111) surface using GGA to DFT with the RPBE and PW91 functional. The calculations carried out in this work significantly expand the database of geometric, energetic and electronic parameters describing carbon adsorption on Fe surface. Most importantly, the dependence of the chemisorption energy on the three sites was quantified and the PDOS were plotted. For carbon adsorption, the relative stabilities were described as follows: hcp hollow $\approx$ fcc hollow $>$ top-on site, whereas the atomic C can not occupy the bridge sites stably. PDOS indicated the strong C(2p)-Fe(3d, 4s+p) and the wide C(2s+p)-Fe(3d) bonding states, which largely confined the electrons of the surface Fe. Comparing the C chemisorptions on γ-Fe and Ni surface at the fcc hollow site, one could see that the number of orbitals at the Fermi level for C adsorbed on γ-Fe(111) is less than on Ni(111). This could imply the weaker catalysis of γ-Fe than Ni for C atom.

[1] G. Glover and C.M. Sellars. Metall. Mater. Trans. B, **4**(3), 765, (1973).

[2] S.J. Pang, T. Zhang, K. Asami and A. Inoue. Acta Mater. **50**(3), 489, (2002).

[3] C. Emmenegger, J.-M. Bonard, P. Mauron, P. Sudan, A. Lepora, B. Grobety, A. Zuttel and L. Schlapbach. Carbon,**41**(3), 539, (2003).

[4] Q. Wu, L.L. Sun, D.Y. Dai, J. Zhang, Z. C. Qin and W. K. Wang. Sci. China Ser. A- Math. **29**(10), 914, (1999).

[5] S. Assabumrungrat, V. Pavarajarn, S. Charojrochkul and N. Laosiripojana. Chem. Eng. Sci. **59**(24), 6015, (2004).

[6] R.B. Anderson, R.A. Friedel and H.H. Storch. J. Chem. Phys. **19**(3), 313, (1951).

[7] F. Fischer, H. Tropsch and Brennst. Chem. **4**, 276, (1923).

[8] D.J. Klinke II, S. Wilke and L.J. Broadbelt. J. Catal. **178**, 540, (1998).

[9] Y.L. Liu, B.W. Yang, F.J. Kong and G. Jiang. Acta Phys. Sin. **56**(9), 5413, (2007).

[10] Y.L. Liu, B.W. Yang and G. Jiang. Acta Phys. -Chim. Sin. **25**(3), 435, (2009).

[11] D.C. Sorescu, D.L. Thompson, M.M. Hurley and C.F. Chabalowski. Phys. Rev. B: Condens. Matter Mater. Phys. **66**(3), 035416, (2002).

[12] D.C. Sorescu. J. Phys. Chem. C, **112**, 10472, (2008).

[13] D. Borthwick, V. Fiorin, S.J. Jenkins and D.A. King. Surf. Sci. **602**, 2325, (2008).

[14] D.E. Jiang and E.A. Carter. Phys. Rev. B, **71**(4), 045402, (2005).

[15] S.J. Jenkins. Surf. Sci. **600**(7), 1431, (2006).

[16] W. Arabczyk, F. Storbeck and H.J. Muessig. Appl. Surf. Sci. **65-66**(1-4), 94, (1993).

[17] W. Arabczyk and U. Narkiewicz. Surf. Sci. **454-456**, 227, (2000).

[18] W. Arabczyk, E. Rausche and F. Storbeck. Surf. Sci. **247**(2-3), 264, (1991).

[19] C. S. Yoo, J. Akella, A. J. Campbell, H. K. Mao and R. J. Hemley. Science, **270**, 1473, (1995).

[20] C. Egawa, S. Katayama and S. Oki. Appl. Surf. Sci. **121/122**, 587, (1997).

[21] Z.Z. Liang, X. Jia,; H.A. Ma, C.Y. Zang, P.W. Zhu, Q.F. Guan, H. Knda. Diamond and Related Materials, **14**(11-12), 1932, (2005).

[22] M.D. Segall, P.J.D. Lindan, M.J. Probert, C.J. Pickard, P.J. Hasnip, S.J. Clark and M.C. Paynel. J. Phys.: Condes. Matter, **14**(11), 2717, (2002).

[23] D. Vanderbilt. Phys. Rev. B, **41**(11), 7892, (1990).

[24] S. G. Louie, S. Froyen and M. L. Cohen. Phys. Rev. B. **26**(4), 1738, (1982).

[25] J.P. Perdew, K. Burke and M. Ernzerhf. Phys. Rev. Lett. **77**(18), 3865, (1996).

[26] J.P. Perdew, J.A. Chevary, S.H. Vosko, K. A. Jackson, M. R. Pederson, D. J. Singh and C. Fiolhais. Phys. Rev. B, **46**(11), 6671, (1992).

[27] B. Hammer, L.B. Hansen and J.K. Norskov. Phys. Rev. B, **59**(11), 7413, (1999).

[28] C.E. Tripa, T.S. Zubkov, J.T. Yates, J. M. Mavrikakis, J. K. N?rskov, J. Chem. Phys. **111**, 8651, (1999).

[29] Y. Zhou, Z. Sun, X. Wang, S. Chen. J. Phys.: Condens. Matter

13, 10001, (2001).
[30] C.F. Huo, J. Ren, Y.W. Li, J.G. Wang and H.J. Jiao. J. Catal. **249**, 174, (2007).
[31] J. Haglund, A.F. Guillermet, G. Grimvall and M. Korling. Phys. Rev. B, **48**(16), 11685, (1993).
[32] M.E. Straumanis and D.C. Kim. Zeitschrift fuer Metallkunde, **60**(4), 272, (1969).
[33] R. Kohlhaas, P. Dunner and N. Schmitz-Pranghe. Zeitschrift Fuer Angewandte Physik, **23**(4), 245, (1967).
[34] A.T. Gorton, G. Bitsianes and T.L. Joseph. Trans. metall. Soc. Aime, **233**(8), 1519, (1965).
[35] B.G. Pfrommer, M. Cote, S.G. Louie and M.L. Cohen. J. Comput. Phys. **131**(1), 233, (1997).
[36] H.W. Leite Alves, J.L.A. Alves, R.A. Nogueira and J.R. Leite. Braz. J. Phys. **29**(4), 817, (1999).